

PACS numbers: 42.65.Jx; 42.70.Hj
DOI: 10.1070/QE2007v037n12ABEH013548

Self-focusing suppression in a system of two nonlinear media and a spatial filter

S.G. Garanin, I.V. Epatko, L.V. L'vov, R.V. Serov, S.A. Sukharev

***Abstract*. It is shown that the rate of development of spatial instability caused by small-scale self-focusing strongly depends on the mutual arrangement of nonlinear media and spatial filters in a setup. The expressions are obtained for the arrangement of elements providing the minimal growth rate of intensity fluctuations. The results of two-dimensional calculations confirm the efficiency of this method of suppressing small-scale self-focusing.**

Keywords: *self-focusing suppression, numerical simulation.*

1. Introduction

The increase in the laser-beam-intensity fluctuations caused by small-scale self-focusing (SSF) is one of the main factors restricting the output parameters of high-power laser setups emitting nanosecond and subnanosecond pulses. Small-scale self-focusing leads to the damage of the elements of laser systems due to a drastic increase in the peak intensity and energy density, causes the degradation of the laser beam quality and increases its divergence.

Various methods of reducing the influence of SSF were analysed in many studies based on the linearized Bespalov – Talanov theory [1] more than a quarter of century ago [2 – 6]. The use of spatial filters (SFs) for retranslating images in optical schemes and filtering high spatial frequencies was considered in [2, 3]. The possibility of suppressing SSF by selecting appropriately telescope parameters was pointed out in [5], and the SSF suppression due the optimal mutual arrangement of elements was studied in [4, 6]. However, the attention of researchers in those years was focused on the analysis of single-pass multistage systems in which each of the stages operated in the nearly limiting regime. This prevented a detailed analysis of the SSF suppression in a simplest system containing two nonlinear media and a SF and the obtaining of quantitative expressions for the optimal arrangement of elements depending on the value of the B integral and angular dimensions of the SF aperture.

Modern high-power facilities [7 – 10] are based on multi-pass amplifiers in which the main phase incursion occurs in the output and preceding elements. The optical schemes include SFs providing the image retranslation and reducing the spatial inhomogeneity of the beam by filtering high spatial frequencies.

At the same time, modern laser facilities are designed by neglecting the possibility of suppressing SSF due to the optimal arrangement of nonlinear elements and SFs, although the laser beams with the smoothed intensity distribution at the periphery used for amplification allow one to move elements quite freely in the scheme by violating the principle of exact retranslation without the appearance of diffraction outbursts at the beam periphery. Simulations of the 12 – 16-kJ four-channel Luch neodymium phosphate glass laser facility by using the Fresnel software package [7] have shown that the rate of spatial instability development caused by SSF depends considerably on the mutual arrangement of amplifiers and SFs in the facility.

In this paper, we considered a simplified problem, determined criteria for the choice of the optimal arrangement of elements, and estimated the reduction of intensity fluctuations. The numerical simulation was used to verify the results obtained for restricted two-dimensional beams in the case of quite strong perturbations and to determine the dependences of the root-mean-square deviation of the beam intensity and the ratio of the peak intensity to the average intensity on the B integral and the angular size of the SF aperture for various mutual arrangements of elements.

2. Optical scheme

We will illustrate the SSF suppression effects by simulating an optical scheme containing two glass rods and two identical SFs. The first SF is mounted in front of the first rod. It restricts the width of the spatial perturbation spectrum at the input to the system. The second SF is mounted between the rods. By changing the position of the second rod with respect to the image of the first rod formed by this SF, we can control the growth rate of perturbations in the system.

The rods were made of glass with the linear and nonlinear refractive indices $n_0 = 1.516$ and $n_2 = 1.1 \times 10^{-13}$ CGSE units, respectively. The length of each of the rods was 300 mm. The typical laser beam diameter for such rods is 40 – 60 mm; however, the suppression effect

S.G. Garanin, L.V. L'vov, S.A. Sukharev Russian Federal Nuclear Center 'All-Russian Research Institute of Experimental Physics', prosp. Mira 37, Nizhnii Novgorod region, 607190 Sarov, Russia;
e-mail: lvov@otd13.vniief.ru;
I.V. Epatko, R.V. Serov A.M. Prokhorov General Physics Institute, Russian Academy of Sciences, ul. Vavilova 38, 119991 Moscow, Russia;
e-mail: epatko@kapella.gpi.ru

Received 22 February 2007
Kvantovaya Elektronika **37** (12) 1159 – 1165 (2007)
Translated by M.N. Sapozhnikov

is independent of the beam diameter. Spatial filters consist of two ideal lenses with a focal distance of 1 m, and the aperture diameter was varied from 2 to 6 mm. The radiation wavelength was 1.053 μm. The average radiation intensity was 3 GW cm^{-2}. For these parameters, the B integral for each nonlinear medium ($B_1 = B_2 = B$) was 1.6 rad. The total B integral for both media is $B_\Sigma = B_1 + B_2 = 3.2$ rad.

3. The Bespalov – Talanov SSF theory (case of small perturbations)

Because most of the papers devoted to SSF studies in laser setups were published a quarter of century ago, we present here the basic expressions obtained in these papers by using the notation accepted in a later paper [11].

The equation for a linearly polarised wave propagating in a medium with the cubic nonlinearity has the form

$$\frac{\partial E}{\partial z} = \frac{1}{2\mathrm{i}k}\,\Delta_\perp E - \mathrm{i}k\gamma E|E|^2, \tag{1}$$

where E is the electric field strength of the wave; $k = 2\pi n_0/\lambda$ is the wave number; λ is the wavelength in vacuum; and $\gamma = n_2/(2n_0)$.

We seek the solution in the form of the harmonic perturbation

$$E = [A_0 + A_1(z)\cos(qx)]\exp\left(-\mathrm{i}k\gamma|A_0|^2 z\right), \tag{2}$$

where A_0 is the unperturbed wave amplitude; q is the transverse wave number of the perturbation; and A_1 is the complex amplitude of the perturbation, which can be represented in the form $A_1 = U + \mathrm{i}V$. The case $V = 0$ corresponds to the amplitude modulation, the case $U = 0$ – to the nearly phase modulation. The modulus of the perturbation amplitude is $|A_1| = (U^2 + V^2)^{1/2}$ and the perturbation phase is $\phi = \arctan(V/U)$.

By assuming that $|A_1| \ll A_0$, we obtain the solution

$$\begin{aligned} U &= U_0\cosh(S\Theta) - \frac{1}{S}\,V_0\sinh(S\Theta), \\ V &= -SU_0\sinh(S\Theta) + V_0\cosh(S\Theta), \end{aligned} \tag{3a}$$

where $U_0 = U(z=0)$; $V_0 = V(z=0)$;

$$\Theta = \frac{q^2}{2k}\,z; \quad S = \left(2\,\frac{B}{\Theta} - 1\right)^{1/2}; \quad B = k\gamma|A_0|^2 z.$$

The quantity B is called the B integral [4] and characterises the phase incursion of the unperturbed beam due to the nonlinear part of the refractive index.

For $B = 0$ (nonlinearity is absent), expressions (3a) are transformed to the solution

$$\begin{aligned} U &= U_0\cos\Theta - V_0\sin\Theta, \\ V &= U_0\sin\Theta + V_0\cos\Theta \end{aligned} \tag{3b}$$

for a linear system.

Let us define the amplitude perturbation transfer coefficient as $K_\mathrm{a}(q,\phi) = |A_1(z)|/|A_1(0)|$. It follows from expressions (3a) that K_a depends on the B integral, the spatial perturbation frequency, and the perturbation phase at the input to a nonlinear medium. Depending on the initial perturbation phase, the perturbation amplitude can either increase or decrease.

For the given spatial frequency, a perturbation with the phase at the input to the nonlinear medium equal to

$$\phi_{\max}^{\mathrm{in}}(q) = \frac{1}{2}\left\{\frac{\pi}{2} + \arctan\left[\frac{\Theta - B}{S\Theta}\tanh(S\Theta)\right]\right\} + \pi m_1 \tag{4a}$$

will increase most rapidly, while a perturbation with the initial phase

$$\phi_{\min}(q) = \phi_{\max}^{\mathrm{in}}(q) - \frac{\pi}{2} + \pi m_2 \tag{4b}$$

will decrease most rapidly, where m_1 and m_2 are arbitrary integers.

The maximum amplitude perturbation transfer coefficient is

$$K_\mathrm{a}^{\max}(q) = K_\mathrm{a}\left(q, \phi_{\max}^{\mathrm{in}}\right) = \frac{B}{S\Theta}\sinh(S\Theta) + \left\{1 + \left[\frac{B}{S\Theta}\sinh(S\Theta)\right]^2\right\}^{1/2}, \tag{5a}$$

and the minimum coefficient is

$$K_\mathrm{a}^{\min}(q) = \frac{1}{K_\mathrm{a}^{\max}(q)}. \tag{5b}$$

It also follows from expressions (3a) that the phase of the perturbation with the maximum growth rate at the output from the nonlinear medium is

$$\phi_{\max}^{\mathrm{out}}(q) = -\frac{\pi}{2} - \phi_{\max}^{\mathrm{in}}(q). \tag{6}$$

We obtain from expression (5a) that for the wave number $q_{\max} = 2[\pi B n_0/(L\lambda)]^{1/2}$ (where L is the nonlinear medium length), the coefficient $K_\mathrm{a}^{\max}(q)$ achieves its maximum equal to $\exp B$. For low spatial frequencies ($q \to 0$), $K_\mathrm{a}^{\max}$ tends to $B + (1 + B^2)^{1/2}$.

The results of papers [2–6] presented above allow us to make the following conclusions.

If a perturbation at the input to the system consists of many spatial harmonics with random phases, the nonlinear medium acts as a filter, by amplifying selectively the harmonics with the phase close to $\phi_{\max}^{\mathrm{in}}(q)$. At the output from the nonlinear medium, the phase of amplified harmonics is not already arbitrary and quite rigorously defined.

For moderate values of the B integral ($B = 1.6$), the maximum transfer coefficients for most rapidly growing perturbations and for low-frequency perturbations differ only by $\sim 30\,\%$. The narrowing of the SF bandwidth will reduce the power of amplified perturbations with the rate that is proportional in fact to the decrease in the area of the SF aperture.

4. Suppression of self-focusing in a system of two nonlinear media

The change in the perturbation amplitude and phase in a system of two identical separated nonlinear media is

described by applying successively expressions (3a), (3b), and again (3a). In this case, if neither a telescope nor a SF is placed between the two nonlinear media in the system under study, the value of Θ in (3a) is calculated by using the distance Δz between the output end of the first nonlinear medium (NM1) and the input end of the second nonlinear medium (NM2). Otherwise, Δz is the distance between the image of the NM1 output end formed by a telescope and the NM2 input end. It was pointed out in [4, 5] that the suppression of self-focusing depends on the perturbed wave phase, however, the optimal conditions for self-focusing suppression were not analysed.

Let us obtain the expression for the optimal distance Δz based on simple considerations. Let us assume that the perturbation phase at the NM1 input is $\phi^{\text{in}}_{\max}(q)$, then, according to (6), the perturbation phase at the NM1 output is $\phi^{\text{out}}_{\max} = -\pi/2 - \phi^{\text{in}}_{\max}(q)$. According to (3b), the perturbation phase at the NM2 input will change by $q^2\Delta z/(2k)$. Let us select the value of Δz so that the condition

$$-\frac{\pi}{2} - \phi^{\text{in}}_{\max}(q) + \frac{q^2\Delta z}{2k} = -\frac{\pi}{2} + \phi^{\text{in}}_{\max}(q) + \pi m \qquad (7)$$

is fulfilled, where m is an integer.

The fulfilment of condition (7) means that the perturbation with the wave number q will decrease in the NM2 and its amplitude at the output from the entire system will be the same as at the system input. By performing calculations using expressions (3a) and (3b), we can see that perturbations with the same spatial frequency but different initial phases in this system also will not increase. Thus, by selecting the distance between nonlinear media, we can suppress self-focusing for any perturbation with the specified spatial frequency. Because the integer factor m in (7) can take arbitrary values, there exists the infinite set of solutions of this equation. Since Δz is defined in the system under study as the distance between the image of the NM1 output end and the NM2 input end, we can consider not only positive but also negative distances Δz. Let us show that one of the solutions at which Δz is negative provides the suppression of self-focusing in a considerably broader range of spatial frequencies compared to all other solutions.

To do this, consider three cases of the NM2 location: directly behind the NM1 output end ($\Delta z = 0$), displaced by $\Delta z = 20$ cm from the NM1 output end, and displaced by $\Delta z = -20$ cm from the image of the NM1 output end. We will consider perturbations with different spatial frequencies by selecting the initial phase of these perturbations so that to provide the maximum rate of their increase in the NM1 [expression (6)]. Figure 1 presents phases calculated at the NM2 input. Curve (*1*) corresponds to the case when the NM2 is located directly behind the NM1, curve (*2*) – to its displacement by $\Delta z = 20$ cm, and curve (*3*) – to its displacement by $\Delta z = -20$ cm.

The dashed curves in Fig. 1 show dependences $\phi^{\text{in}}_{\max}(q)$ [expression (4a)], which we will call the 'most dangerous' phase curves. The dotted curves presents dependences $\phi_{\min}(q)$ [expression (4b)], which we will call the 'desirable' phase curves. Note that both the 'most dangerous' and 'desirable' phase curves have the negative derivative with respect to the spatial frequency.

One can see that curves (*1–3*) begin from one point in the region of low spatial frequencies, but curves (*1*) and (*2*) have positive derivatives and intersect both the 'desirable' phase and 'most dangerous' phase curves. Perturbations with the spatial frequencies determined by points of intersection of curves (*1–3*) with the 'desirable' phase curves will not be amplified in the system under study. Perturbations with the spatial frequencies determined by points of intersection with the 'most dangerous' phase curves have the maximum transfer coefficient. Curve (*3*) has the negative derivative and is close to one of the 'desirable' phase curves in a rather broad spatial frequency range.

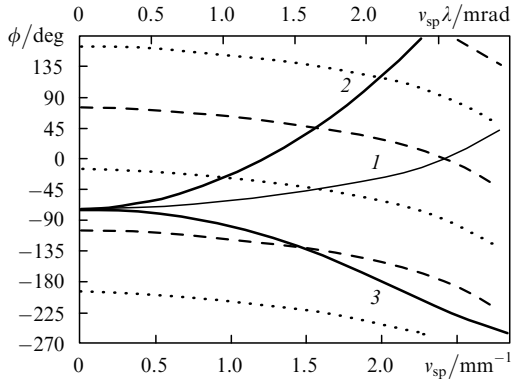

Figure 1. Dependences of the perturbation-wave phase at the NM2 input on the spatial perturbation frequency $v_{sp} = q/2\pi$ and the quantity $v_{sp}\lambda$ (for $\lambda = 1.053$ μm) for different locations of nonlinear media: the image of the NM1 output end coincides with the NM2 input end (or the two rods are mounted close to each other) (*1*); the distance between the NM1 output end and the NM2 input end is $\Delta z = 20$ cm (*2*); the distance between the image of the NM1 output end and the NM2 input end is $\Delta z = -20$ cm (*3*). The dashed and dotted curves are the 'desirable' and 'most dangerous' phases, respectively.

Figure 2 presents the dependences of the maximum perturbation transfer coefficient on the spatial frequency for the same three cases of the mutual arrangement of the NM1 and NM2. The shape of the curves considerably depends on the distance between the nonlinear media. One can see that, both for the positive and negative displace-

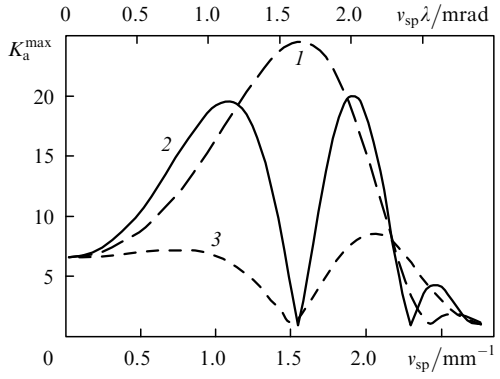

Figure 2. Dependences of the maximum perturbation transfer coefficient $K_a^{\max}$ on the spatial perturbation frequency $v_{sp} = q/2\pi$ and the quantity $v_{sp}\lambda$ (for $\lambda = 1.053$ μm) in a system of two nonlinear media and a SF without an aperture (telescope) for different locations of nonlinear media: the image of the NM1 output end coincides with the NM2 input end (or the two rods are mounted close to each other) (*1*); the distance between the NM1 output end and the NM2 input end is $\Delta z = 20$ cm (*2*); the distance between the image of the NM1 output end and the NM2 input end is $\Delta z = -20$ cm (*3*).

ments Δz according to Fig. 1, the spatial frequency exists for which $K_a^{max} = 1$. For positive displacements Δz, a sharp dip appears in curve (*2*) (Fig. 2); however, its width is relatively small. For the negative displacement of the NM2 with respect to the NM1, the perturbation transfer coefficient becomes considerably smaller in the entire spatial frequency range compared to other cases.

The optimal displacement depends on the transmission band of the SF and the shape of the spatial perturbation spectrum. If the condition $K_a^{max}(q) = 1$ should be provided for the specified $q = q_1$, the optimal solution of Eqn (7) is written in the form

$$\Delta z = \frac{4k}{q_1^2}\,\phi_{max}^{in}(q_1). \tag{8a}$$

If the SF has an aperture of angular size $\varphi_{lim} \leqslant k/q_{max}$, the optimal displacement in the case of the uniform spatial perturbation spectrum can be determined from the semi-empirical expression

$$\Delta z \approx -\frac{L}{n_0}\frac{\arctan B}{B} + \frac{\lambda}{\pi(0.85\varphi_{lim})^2}\left(\arctan B - \frac{\pi}{2}\right). \tag{8b}$$

This expression was derived by interpolating the dependence $\phi_{max}^{in}(q)$ by a parabola and setting q_1 equal to $0.85\varphi_{lim}k$. By substituting the parameters of the nonlinear medium into (8b), we obtain the optimal displacement equal to -24 cm for the angular aperture size of 1.5 mrad and to -38 cm for 1 mrad.

Thus, the linearized Bespalov–Talanov theory in the small perturbation approximation predicts that SSF in a system of two nonlinear media and a SF can be considerably suppressed by the proper mutual arrangement of the elements.

Mathematical simulations allow the verification of this prediction for the large perturbation amplitudes of spatially restricted beams. The calculations of two-dimensional intensity distributions give the evolution of the peak intensity and its root-mean-square deviation from the average value during the beam propagation.

5. Simulation of the transverse instability during self-focusing of real beams

5.1 Brief characteristic of the model

Simulations were performed by using the Fresnel software package. The parabolic equation was solved in the paraxial approximation by using a series of Fourier transforms. A laser beam is specified by a three-dimensional set of complex numbers describing the spatial and time distributions of the electric-field amplitude and phase. The set can contain up to 2^{27} elements. Depending on the problem being solved, sets of sizes $1 \times 8192 \times 8192$, $8 \times 4096 \times 4096$, $32 \times 2048 \times 2048$, etc, were used. The first number is the number of time steps, and the two next numbers are the numbers spatial steps.

Nonlinear-optical elements were simulated by the method of step-by-step separation in which a homogeneous medium is divided into a number of infinitely thin nonlinear layers separated by vacuum gaps [12]. To obtain correct results, the maximum phase increment in any nonlinear layer should not exceed 0.1–0.2 rad. The Fresnel program takes into account the influence of linear and nonlinear losses, the intensity amplification in the active medium, and the change in the pulse shape caused by amplification saturation. However, to simplify analysis, we do not consider all these effects in this paper.

5.2 The input intensity distribution

The input beam was specified as a restricted beam with a flat top and power P modulated by the amplitude by the Gaussian noise of power P_{noise} with the uniform on average spectral distribution in the specified band. The far-field noise intensity distribution (angular spectrum) represents a speckle pattern with the characteristic angular sze λ/D (where D is the beam size). The term 'uniform on average' means that after the azimuthal averaging, the far-field noise intensity is independent of the angle between the propagation directions of the main wave and the noise component. The maximum angle of deviation of the propagation direction of the noise wave from the main beam axis is 1.5 rad, the minimum near-field speckle size being 0.7 mm.

We will characterise the beam inhomogeneity by the ratio of the peak intensity to the average intensity I_{peak}/I_{av}. Although this quantity is very important for determining the probability of damaging optical elements, we are aware of only one paper [13] in which the empirical expression was presented for calculating this ratio in the laser system with SSF. To estimate correctly the peak intensity in simulations, it is necessary to obtain a considerable calculation statistics. In [13, 14], the beam inhomogeneity was characterised by the so-called contrast rms_I/I_{av}, where rms_I is the root-mean-square deviation of the beam intensity. This quantity can be estimated by using smaller samplings. The values of rms_I/I_{av} and I_{peak}/I_{av} for the input intensity distribution are described with good accuracy by the expressions

$$\mathrm{rms}_I/I_{av} = \left[1 + \left(\frac{P_{noise}}{P}\right)^{1/2}\right]^2 - 1, \tag{9a}$$

$$I_{peak}/I_{av} = \left[1 + c\left(\frac{P_{noise}}{P}\right)^{1/2}\right]^2, \quad c \approx 5. \tag{9b}$$

The maximum size of the calculation network was 8192×8192 points, the sampling step was 0.063 mm, and the modulated-beam diameter was 42 cm. This diameter greatly exceeds real beam diameters in the system under study, which allowed us to replace in simulations the statistics over realisations by spatial statistics. The sampling step is an order of magnitude smaller than the minimum speckle size, which also provides the high calculation accuracy.

5.3 Results of simulation

The peak intensity I_{peak} is the greatest intensity in the given cross section of the beam. Let us define the maximum intensity I_{max} as the greatest peak intensity over the entire propagation path of the beam.

We determined in two-dimensional calculations the peak beam intensity in many cross sections along the propagation path from the input to the NM1 up to a distance of $Z \approx$ 2 m from the NM2 output. Of most practical interest is the peak intensity at the NM2 output and the maximum peak intensity in a plane located behind the NM2. The former

determines the NM2 damage probability, while the latter determine the damage of an optical element that can be found in this plane. Figure 3a shows the change of the peak intensity of the modulated beam propagating in the NM2 and behind it. The beam evolution (with a random noise component) during self-focusing occurs in the following way: the beam intensity achieves a local maximum at one of the points of the beam cross section and then begins to decrease, while at another random point at a distance of Z the beam intensity becomes maximal over the entire beam cross section, etc. These points are often separated by a great distance in the beam cross section, and therefore the peak intensities for different distances Z can correspond to points with different coordinates in the beam cross section.

The fraction of the noise field component at the NM1 input is $P_{\text{noise}}/P = 9 \times 10^{-5}$, $I_{\text{peak}}/I_{\text{av}} = 1.1$ (the contrast is 0.0185). The zero coordinate Z corresponds to the NM2 input, and the plane $Z = 30$ cm – to the NM2 output. The dashed curve is plotted for a system without self-focusing suppression, in which the image of the NM1 output end coincides with the NM2 input end. In this case, the beam peak intensity increases continuously in the NM2 ($Z = 0-30$ cm) and exceeds the average intensity by 2.8 times at the NM2 output. The peak intensity continuous to increase behind the NM2 and achieves its maximum at a distance of 5 cm ($Z = 35$ cm) from the NM2 boundary. The peak intensity in this plane exceeds the average intensity by 3.4 times. The continuation of the increase in the peak intensity during linear propagation is related to the shape of the beam wavefront at the NM2 output. In the region of main intensity peaks, the wavefront converges, while in the region of intensity minima, it diverges. This results in the increase in the intensity contrast and increase in the peak intensity during beam propagation.

We will optimise the nonlinear system by decreasing the maximum intensity $I_{\max}$. Our calculations showed that the optimal displacement for the nonlinear system is $\Delta z = -24$ cm. This value agrees with expression (8b). The solid curve in Fig. 3a corresponds to a system with self-focusing suppression, when the NM2 is displaced by 24 cm toward a SF. This dependence shows that the maximum beam intensity for the optimal system is considerably lower than that for a system without self-focusing suppression and nowhere exceeds 1.36 of the average intensity. This intensity ratio at the NM2 output is 1.13, coinciding in fact with the value 1.1, which was specified at the nonlinear-medium input. For systems with the optimal self-focusing suppression, the peak intensity typically decreases during beam propagation in the NM2 until some plane (see Fig. 2). Then, when the self-focusing effect in the NM2 becomes dominant, the peak intensity begins to increase, which is continued behind the NM2.

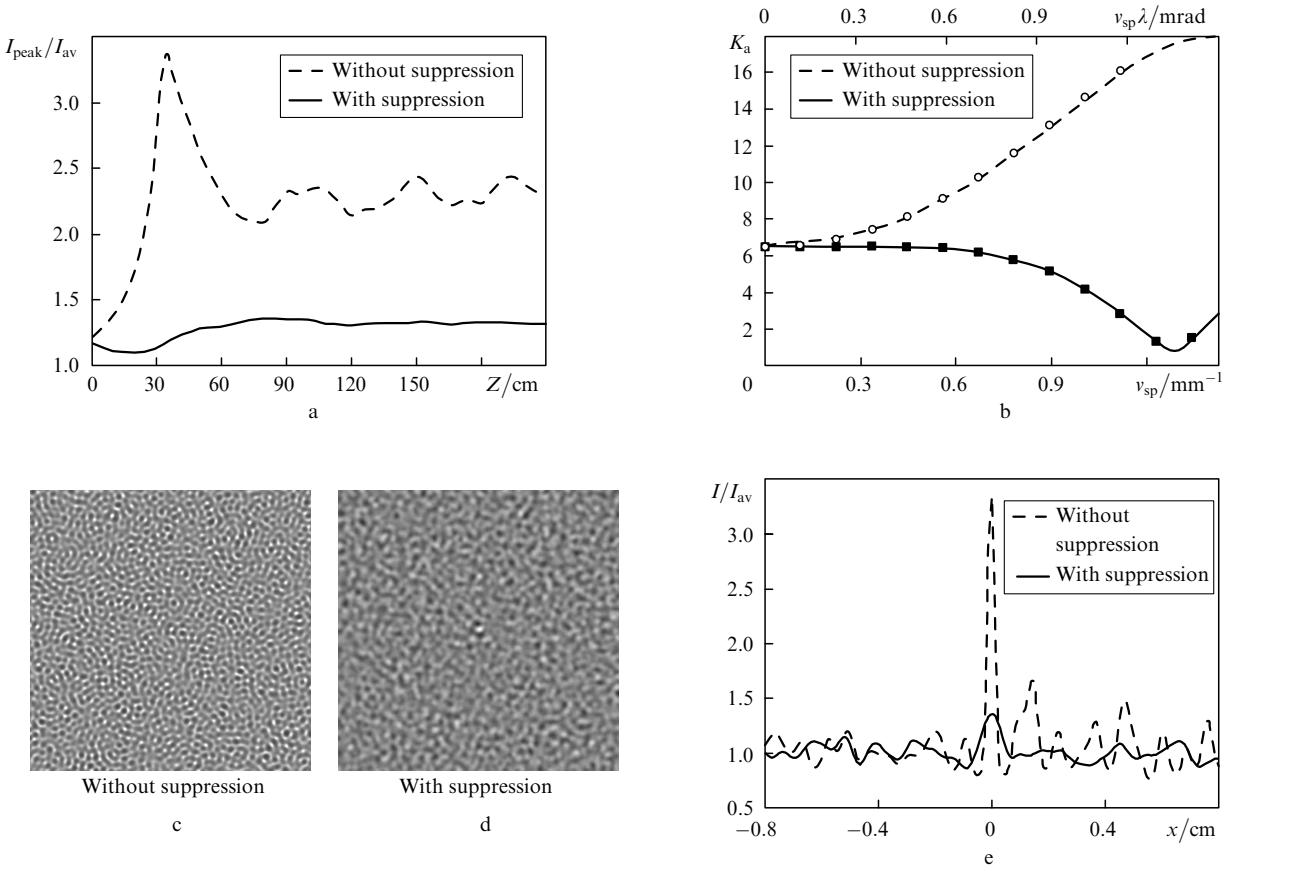

Figure 3. Results of two-dimensional numerical simulations: the evolution of the peak-to-average beam intensity ratio during the propagation of radiation behind the system of two nonlinear media (a); dependences of the perturbation transfer coefficient on the spatial frequency v_{sp} and the quantity $v_{\text{sp}}\lambda$ in systems without and with self-focusing suppression (curves are the results of simulation, points are predicted by the linearized Bespalov–Talanov theory) (b); spatial intensity distributions in systems without and with self-focusing suppression in planes $Z = 35$ and 80 cm, respectively, corresponding to the maximum peak intensity (c, d); and cross sections of the intensity distribution in planes $Z = 35$ and 80 cm passing through the brightest point of each of the distributions (e).

Figure 3b presents the dependences of the transfer coefficient K_a of the noise component on the spatial frequency after propagation through the nonlinear system. The curves show the results of the two-dimensional simulation of self-focusing, and points are predicted by the linearized Bespalov – Tolanov theory. One can see that even in the system without self-focusing suppression, when the maximum noise amplitude is almost equal to the average amplitude of the beam field, the linearized theory well predicts the amplitude transfer coefficient.

Figures 3c and 3d present the fragments of two-dimensional intensity distributions for the system without and with self-focusing suppression in planes $Z = 35$ and 80 cm, respectively, and Fig. 3d shows the cross sections of these distributions passing through the brightest point of each of the distributions.

The results of simulation show that the contrast and maximum intensity at the nonlinear-system output are determined by the noise energy, which increases due to self-focusing. Let us introduce the effective transfer coefficient κ_{eff} for the nonlinear system. The quantity $\kappa_{\text{eff}}^2 P_{\text{noise}}$ describes the power density that increased due to self-focusing after the beam propagation through the nonlinear system. The two-dimensional calculations showed that the quantities $\text{rms}_I/I_{\text{av}}$ and $I_{\max}/I_{\text{av}}$ at the system output can be approximately described by the expressions

$$\text{rms}_I/I_{\text{av}} = \left[1 + \kappa_{\text{eff}}\left(\frac{P_{\text{noise}}}{P}\right)^{1/2}\right]^2 - 1, \tag{10a}$$

$$I_{\max}/I_{\text{av}} = \left[1 + c\kappa_{\text{eff}}\left(\frac{P_{\text{noise}}}{P}\right)^{1/2}\right]^2, \quad c \approx 5. \tag{10b}$$

In the system without self-focusing suppression, κ_{eff} tends to $\exp(0.9B_\Sigma)$ when the SF transmission band is comparable with $q_{\max}$, and to $B_\Sigma + (1 + B_\Sigma^2)^{1/2}$ when the SF transmission band is narrower than $q_{\max}/3$. In the system with the restricted SF transmission band, narrower than $q_{\max}$, and for the optimal negative displacement of the NM2 with respect to the NM1 determined by expression (8b), we have $\kappa_{\text{eff}} \approx 0.5[B_\Sigma + (1 + B_\Sigma^2)^{1/2}]$.

Unlike the empirical relations used in [13, 4], expressions (10) have a simple physical meaning and take into account the influence of the angular size of the SF aperture, the mutual arrangement of elements, and the values of initial perturbations.

Fresnel simulations showed that self-focusing suppression in a system of two nonlinear media and a SF is preserved for a quite large ratio $I_{\text{peak}}/I_{\text{av}} = 1.22$ at the system input. In this case, as follows from two-dimensional calculations (Fig. 4), the peak intensity in the system with self-focusing suppression exceeds the average intensity by 1.44 times, and the maximum intensity exceeds the average intensity by 1.9 times. In the system without self-focusing suppression for the same input noise level, self-focusing leads to the catastrophic increase in the beam intensity inside the NM2 at a distance of 24 cm from the input end, resulting in the damage of the medium.

In conclusion, we summarise in Table 1 the results of two-dimensional SSF calculations for a beam with the noise modulation.

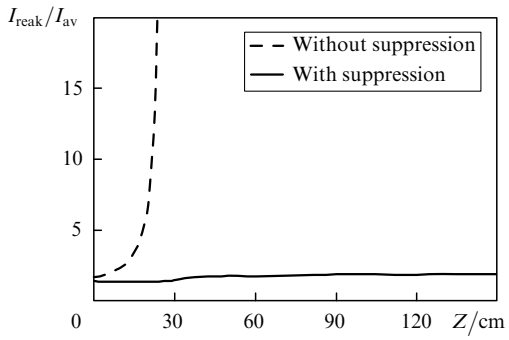

Figure 4. Development of self-focusing in a system. At the system input: $P_{\text{noise}}/P = 4 \times 10^{-4}$, contrast is 0.041, and $I_{\text{peak}}/I_{\text{av}} = 1.22$.

Table 1.

System	$I_{\text{peak}}/I_{\text{av}}$ (at the input)	$I_{\text{peak}}/I_{\text{av}}$ (at the NM2 output)	$I_{\max}/I_{\text{av}}$
Without suppression	1.1	2.8	3.4
With suppression		1.13	1.36
Without suppression	1.22	Medium damage	–
With suppression		1.44	1.9

6. Conclusions

We have shown that the peak intensity outbursts caused by self-focusing in a system consisting of two nonlinear media and a spatial filter can be considerably reduced by providing the optimal mutual arrangement of these media and the filter between them. The optimal displacement depends on the parameters of nonlinear media and the shape of the spatial perturbation spectrum.

The expressions relating the maximum intensity and contrast after self-focusing with the parameters of the nonlinear system and the input noise power are presented.

The suppression of self-focusing considerably improves the reliability of multichannel high-intensity laser facilities. To determine the possibility of a further increase in the average output intensity, it is necessary to study the effect of nonlinear imaging (hot image) and the influence of the gain saturation in the active medium on self-focusing.

References

1. Bespalov V.I., Talanov V.I. *Pis'ma Zh. Eksp. Teor. Fiz.*, **3**, 307 (1966).
2. Hunt J.T., Glaze J.A., Simmons W.W., Renard H.F. *Appl. Opt.*, **17**, 2053 (1978).
3. Holzrichter J.F., Eimerl D., George E.V., Trenholme J.B., Simmons W.W., Hunt J.T. *LLNL. Physics of Laser Fusion. Vol. III. High Power Pulsed Lasers, UCRL-52868, Rev 1* (Livermore, Cal, 1982) pp 31 – 35.
4. Rozanov N.N., Smirnov V.A. *Kvantovaya Elektron.*, **7**, 410 (1980) [*Sov. J. Quantum Electron.*, **10**, 232 (1980)].
5. Vlasov S.N., Yashin V.E. *Kvantovaya Elektron.*, **8**, 510 (1981) [*Sov. J. Quantum Electron.*, **11**, 313 (1981)].
6. Babichenko S.M., Bykovskii N.E., Senatskii Yu.V. *Kvantovaya Elektron.*, **9**, 161 (1982) [*Sov. J. Quantum Electron.*, **12**, 105 (1982)].
7. Van Wonterghem B.M., Barker C.E., Murray J.R., Smith I.C., Campbell J.H., Browning D.F., Speck D.R., Behrendt W.C. *LLNL. ICF Quarterly Report UCRL-LR-105821-95-1* (Livermore, Cal, 1995) pp 1 – 17.

8. Miller G.H., Moses E.I., Wuest C.R. *Opt. Eng.*, **43**, 2841 (2004).
9. Garanin S.G., Zaretskii A.I., Il'kaev R.I., Kirillov G.A., Kochemasov G.G., Kurunov R.F., Murugov V.M., Sukharev S.A. *Kvantovaya Elektron.*, **35**, 299 (2005) [*Quantum Electron.*, **35**, 299 (2005)].
10. Andre M.L. *Proc. SPIE Int. Soc. Opt. Eng.*, **3047**, 38 (1997).
11. Sacks R.A., Henesian M.A., Haney S.W., Trenholm J.B. *LLNL. ICF Quarterly Report UCRL-LR-105821-96-4* (Livermore, Cal, 1996) pp 207 – 213.
12. Williams W., Trenholme J.B., Orth C., Haney S.W., Sacks R.A., Auerbach J., Lawson J., Henesian M., Jancaitis K., Renard P. *LLNL. ICF Quarterly Report UCRL-LR-105821-96-4* (Livermore, Cal, 1996) pp 181 – 191.
13. Williams W.H., Auerbach J.M., Henesian M.F., Lawson J.K., Hunt J.T., Sacks R.A., Widmayer C.C. *Proc. SPIE Int. Soc. Opt. Eng.*, **3264**, 93 (1998).
14. Wegner P., Van Wonterghem B.M., Burkhart S., Widmayer C.C., Murray J.R. *LLNL. ICF Quarterly Report UCRL-LR-105821-99-1* (Livermore, Cal, 1996) pp 43 – 61.